J. Cell. Mol. Med. Vol 13, No 2, 2009 pp. 398-409

Progressive silencing of p14ARF in oesophageal adenocarcinoma

Yinghui Huang [a, b, *], Christopher J. Peters [b], Rebecca C. Fitzgerald [b], Ruth A. Gjerset [a, *]

[a] Sidney Kimmel Cancer Center, Cancer Cell Biology, San Diego, CA, USA
[b] MRC Cancer Cell Unit, Hutchison-MRC Research Centre, Cambridge, and Addenbrooke's Hospital, Cambridge University Hospitals NHS Foundation Trust, Cambridge, United Kingdom

Received: November 16, 2007; Accepted: March 24, 2008

Abstract

The frequency of oesophageal adenocarcinoma is increasing in Western countries for unknown reasons, and correlates with a corresponding increase in the pre-malignant condition, Barrett's Oesophagus, which raises the risk of adenocarcinoma by some 40- to 125-fold. We have examined how disease progression correlates with changes in expression of the p14ARF (ARF) tumour suppressor, a key regulator of the p53 tumour suppressor pathway that is silenced in some 30% of cancers overall, but for which a role in oesophageal cancer is unclear. We have used quantitative PCR, RT-PCR, methylation-specific PCR and chromatin-immunoprecipitation to examine the regulation and function of ARF in oesophageal adenocarcinoma tissue specimens and cell lines. We find highly significant reductions ($P < 0.001$) in ARF expression during disease progression from normal oesophageal epithelium to Barrett's Oesophagus to adenocarcinoma, with 57/76 (75%) adenocarcinomas displaying undetectable levels of ARF expression. Retention of ARF expression in adenocarcinoma is a highly significant indicator of increased survival ($P < 0.001$) and outperforms all clinical variables in a multivariate model. CpG methylation as well as histone H3 methylation of lysines 9 and 27 contribute independently to ARF gene silencing in adenocarcinoma cell lines and can be reversed by 5-aza-2′-deoxycytidine. The results suggest that silencing of ARF is involved in the pathogenesis of oesophageal adenocarcinoma and show that either DNA or histone methylation can provide the primary mechanism for ARF gene silencing. Silencing of ARF could provide a useful marker for increased risk of progression and poor prognosis.

Keywords: p14ARF • oesophageal adenocarcinoma • Barrett's oesophagus • CpG methylation • histone methylation

Introduction

The incidence of oesophageal adenocarcinoma (AC), for which the 5-year survival rate is 13.6% [1], has increased in the United States and Western countries for poorly understood reasons over the past three decades. Early detection is critical to treatment success, and is based on endoscopic surveillance of dysplasia in the pre-malignant condition, Barrett's oesophagus (BE), characterized by metaplastic columnar oesophageal epithelial cells. BE increases the risk of AC by some 40- to 125-fold [2], and provides an opportunity for early intervention. Several studies have identified genes or gene expression patterns that are characteristic of BE or AC [3–5], and several markers identify patient subsets at high risk for progression, including aneuploidy, p53 loss of heterozygosity and p16INK4a (CDKN2A) abnormalities [6–8]. However, not all patients with these abnormalities progress, and there is therefore a need to identify additional indicators of risk.

The p14ARF tumour suppressor (hereafter referred to as 'ARF', for Alternate Reading Frame) is estimated to be silenced in some 30% of cancers overall [9], making it one of the most frequently altered genes in human cancer, and a possible indicator of progression. ARF plays a well-established role in activating the p53 tumour suppressor pathway in response to oncogenic hyperproliferative signals [10], and in addition engages in less well-understood p53-independent functions [11–14]. In AC, the specific role of ARF gene silencing has not been addressed, and CpG methylation of ARF, a common mechanism of tumour suppressor gene silencing in cancer [15], has been observed in tumour specimens with variable

*Correspondence to: Ruth A. GJERSET,
Sidney Kimmel Cancer Center, 10905 Road to the Cure,
San Diego, CA 92121, USA.
Tel.: 858-450-5990 ×232; Fax: 858-450-3251
E-mail: rgjerset@skcc.org,

doi:10.1111/j.1582-4934.2008.00336.x

frequencies in different studies, up to about 30% [16–18]. The possibility that disease progression could involve quantitative changes in ARF expression levels, and the possible involvement of other silencing mechanisms such as histone modifications has not been examined. We have therefore used clinical specimens of normal oesophageal epithelium (NE), BE, and AC, and early passage cell lines derived from these tissue types, to examine possible changes in ARF expression during disease progression, as well as molecular mechanisms that may be involved.

Materials and methods

Cell culture

Barrett's and oesophageal cell lines that closely model the tissue of origin [19–21] and were at early passage (less than passage 20) were maintained at 37°C in 10% CO_2 in DMEM supplemented with nonessential amino acids, pyruvate, L-glutamine, gentamicin, and 10% FBS, except for Gohtert, Gihtert, Chtert and Het1A, for which 20% FBS was added. Table 1 lists the cell line characteristics and source.

Tissue specimens

Twenty biopsies of normal squamous oesophagus (in patients without Barrett's oesophagus) and 20 biopsies of Barrett's oesophagus were collected from Addenbrooke's Hospital in Cambridge (by R.C.F.) and University College Hospital in London, in collaboration with Dr. Laurence Lovat. Histological diagnosis was verified by pathological examination of paired biopsies taken for clinical purposes from the same endoscopic site. The 76 adenocarcinoma samples were pre-treatment biopsies obtained from Professor Hugh Barr at Gloucester NHS Trust and Professor Derek Alderson at Bristol Royal Infirmary. Patients were subsequently treated with esophagectomy. For all adenocarcinoma samples, histology was confirmed on a frozen section taken from the research specimen by two independent pathologists (Professor Neil Shepherd and Professor Brian Warren for Gloucester samples and the reporting clinical pathologist in addition to Dr. Vicki Save for Bristol samples). All the samples were taken from the lower part of oesophagus, 2 cm above the oesophago-gastric junction, and were processed for research if epithelial cellularity was >80%. Ethics Committee approvals from each participating institution were obtained for these studies, and written informed consent was obtained from the participating patients.

RT-PCR and PCR

Total RNA or DNA prepared from cells or frozen tissue using Triozol Reagent (Invitrogen, Carlsbad, CA, USA) according to the protocol supplied by the manufacturer was subjected to RT-PCR or PCR, respectively, using primers chosen to amplify a gene fragment of about 300–600 bases. Primers were synthesized by Sigma (Genosys, Woodlands, TX, USA) and are listed in Table 2. The conditions used were as follows: 95°C (2 min.), followed by 40 cycles of 95°C (30 sec.), 58°C (30 sec.) and 72°C (30 sec.).

Methylation-specific PCR (MSP)

CpG island methylation analysis was determined using bisulphite-treated genomic DNA following the instructions of EZ DNA methylation kit (Zymo research, Orange, CA, USA). Primers specific for the methylated strand (M) and unmethylated strand (U) of the ARF promoter/exon1β were used, and were designed to include 5 CpG sites and 9 CpG sites in the M and U primers, respectively, in order to maximize specificity. Positive and negative controls were carried out using *in vitro* CpG methylated human sperm DNA with *Sss*I (CpG) methylase (New England Biolabs, Inc., Beverly, MA, USA) or unmethylated sperm DNA, respectively. The primer sequences are listed in Table 2, and conditions were as described for RT-PCR. Methylated sites within the PCR amplified regions were determined by sequencing the purified MSP products.

Q-PCR and Q-MSP

Real-time quantitative PCR (Q-PCR) was optimized by melt-curve analysis, and efficiency was calculated by serial dilutions. ARF-expressing BJ-1 cells and ARF-null TE7 cells were used as positive and negative controls, respectively. cDNA prepared from tissue or cellular RNA was diluted 1:10 and 5 μl was amplified in a 20 μl volume (in triplicate) containing 10 μl of Sigma SYBR Green PCR Master Mix (Sigma-Aldrich) and 0.2 μmol/l final concentration of each primer, using a Rotor-Gene 3000 Real-time PCR cycler (Westburg Genomics, the Netherlands), using conditions described for RT-PCR. Gene expression was measured relative to GAPDH (glyceraldehyde phosphate dehydrogenase) and was expressed as Relative Transcript Abundance = $1000/2^{(CT\ \mathrm{ARF}\ -\ CT\ \mathrm{GAPDH})}$, where C_T = threshold cycle. The primers for ARF and GAPDH were the same as those described for RT-PCR and are listed in Table 2, and conditions were as described for RT-PCR.

Quantitative MSP (Q-MSP) analysis of bisulphite-treated DNA was performed similarly (in triplicate). The levels of unmethylated and methylated species were determined by a standard curve constructed by serial dilutions of unmethylated or *Sss*I-methylated human sperm DNA, respectively. Dilution experiments showed linearity of amplification down to a dilution of $1{:}10^4$ for methylated DNA as well as for unmethylated DNA. The primers used were the same as for MSP and are listed in Table 2, and PCR conditions were as described for RT-PCR.

Bisulphite sequencing

Two micrograms genomic DNA was bisulphite-treated and used for PCR amplification of a 270 base pair region with universal primers listed in Table 2, and conditions described for RT-PCR. The PCR product was gel-purified and sequenced using the same primers.

Chromatin immunoprecipitation (ChIP)

ChIP assays were performed following the chromatin immunoprecipitation protocol on the Upstate website (www.upstate.com). Two micrograms of anti-trimethyl-histone H3 (Lys-9) antibody (07–442, Upstate, USA) and anti-dimethyl-histone H3 (lys-9) antibody (ab7312, shared epitope with H3-lys-27, Abcam, UK) was used for each ChIP reaction. ARF sequences in the immunoprecipitates and starting material (input) were detected by PCR using ARF ChIP primers listed in Table 2, and conditions described for RT-PCR.

Table 1 Cell lines

Cell line	Description	Source	p53 status**
HET1A	Normal human epithelial cells immortalized with SV40 T-antigen	American Type Culture Collection (ATCC)	Wild-type
BJ-1	Normal human fibroblast cells immortalized with human telomerase	American Type Culture Collection (ATCC)	Wild-type
OE33	Oesophageal adenocarcinoma	European Collections of Cell Cultures (ECACC)	Codon 135, TGC(cys)→TAC(tyr)
TE7	Oesophageal adenocarcinoma***	Dr. T. Nishihira, Kurokawa County Hospital, Japan	Null
SEG1	Oesophageal adenocarcinoma	Dr. D.G. Beer, University of Michigan, USA	Wild-type
FLO	Oesophageal adenocarcinoma	Dr. D.G. Beer, University of Michigan, USA	Codon 277, TGT(cys)→TTT(phe)
OC1	Oesophageal squamous cell carcinoma	Dr. O'Sullivan, Cork Cancer Center, Ireland	Wild-type
OC3	Oesophageal adenocarcinoma	Dr. O'Sullivan, Cork Cancer Center, Ireland	Codon 244, GGC(gly)→GAC(asp)
Gihtert*	Barrett's oesophagus cells immortalized with human telomerase	Dr. J. Anderson, University of Washington, USA	Codon 248, CGG(arg)→TGG(trp)
(CP-C)			
Gohtert*	Barrett's oesophagus cells immortalized with human telomerase	Dr. J. Anderson, University of Washington, USA	Codon 302, GGG(gly)→ GG- (frameshift)
(CP-D)			
Chtert*	Barrett's oesophagus cells immortalized with human telomerase	Dr. J. Anderson, University of Washington, USA	Codon 175, CGC(arg)→CAC(his)
(CP-B)			

*(1) Barrett, M. T., *et al.* Cancer Res, *63:* 4211–4217, 2003; (2) Palanca-Wessels, M. C., *et al.* Carcinogenesis, *24:* 1183–1190, 2003.
**Determined by RT-PCR sequencing of exons 5–9.
***Presently used lines likely to be of oesophageal squamous cell origin (Boonstra *et al.*, Cancer Res. *67:* 7996–8001, 2007).

Statistical analyses

The significance of differences in ARF expression data in tissue specimens was determined by a Kruskal-Wallis rank sum test. Kaplan–Meier survival curves were evaluated by a Log Rank (Mantel-Cox) test. For multivariate analysis, a Cox regression model using a backward stepwise method was utilized. Fisher's exact test was used to determine if the ARF expression status was associated with the N-Stage of the tumour.

Results

ARF expression and gene status in clinical specimens

ARF expression was examined by quantitative PCR (Q-PCR) in prospectively collected clinical specimens of oesophageal tissue from individuals with a normal squamous oesophagus (20 specimens) and patients with non-dysplastic BE (20 specimens) or AC (76 specimens). We found highly significant decreases in ARF expression ($P < 0.001$) with disease progression from normal oesophageal epithelium (NE), to non-dysplastic BE to AC (Fig. 1A). Furthermore, 57 of 76 (75%) AC specimens had undetectable levels of ARF expression, while only 4 of 20 (20%) BE specimens and none of the NE specimens displayed undetectable levels of ARF expression. Table 3 summarizes the ARF expression analysis for the 47 AC specimens for which follow-up data were available.

Correlation of ARF expression with clinical outcome

Among the 76 AC patients whose tumours were analysed for ARF expression in Figure 1A, clinical data relating to disease stage and survival were available for 47 patients (Table 3). Only T-stage (Log rank Mantel-Cox test, $\chi^2 = 7.65$, d.f. = 2, $P = 0.022$), and ARF

Table 2 Primer sequences

Primer name	Application	Sequence
ARF-forward	RT-PCR	5′-ATGGGCAGGGGGCGGTGCGT-3′
ARF reverse	RT-PCR	5′-TCAGCCAGGTCCACGGGCAGA-3′
GAPDH-forward	RT-PCR	5′-GAAGGTGAAGGTCGGAGTC-3′
GAPDH-reverse	RT-PCR	5′-GAAGATGGTGATGGGATTTC-3′
ARF exon1β-forward	PCR	5′-TGGGTCCCAGTCTGCAGTTA-3′
ARF exon 1ß-reverse	PCR	5′-GGCTCCTCAGTAGCATCAGC-3′
ARF exon 2-forward	PCR	5′-CACTCTCACCCGACCCGT-3′
ARF exon 2-reverse	PCR	5′-ACCTTCCGCGGCATCTAT-3′
M-forward	MSP	5′-GTCGAGTTCGGTTTTGGAGG-3′ (-30 from translation start)*
M-reverse	MSP	5′-AAAACCACAACGACGAACG-3′ (133 from translation start)*
U-forward	MSP	5′-TGAGTTTGGTTTTGGAGGTGG-3′ (-28 from translation start)*
U-reverse	MSP	5′-AACCACAACAACAAACACCCCT-3′ (131 from translation start)*
ARF ChIP Forward	ChIP	5′-ATGGGCAGGGGGCGGTG-3′ (-123 from translation start)*
ARF ChIP Reverse	ChIP	5′-CTGGTCTTCTAGGAAGCGGCT-3′ (192 from translation start)*
ARF universal forward	Bisulphite sequencing	5′-TTGTTTATTTTTGGTGTTAAAGGG-3′ (-67 from start)*
ARF universal reverse	Bisulphite sequencing	5′-CCTTTCCTACCTAATCTTCTAAAAAAC-3′ (+203 from start)*

*The 5′ position of the primers relative to the start of translation (base pair 161 of GenBank sequence number NM_058195) is indicated in parentheses.

expression (Log rank Mantel-Cox test, χ^2 = 21.69, d.f. = 1, P < 0.0001, see Fig. 1B) were prognostically significant on univariate analysis, though the N-Stage approached statistical significance (Log rank Mantel-Cox test, χ^2 = 3.72, d.f. = 1, P = 0.052). Retaining ARF expression significantly improved survival, and even low levels of ARF seemed to provide a barrier to tumourigenic progression. When entering differentiation, T-stage, N-stage and ARF expression status into a Cox regression model, only ARF expression remained outperforming all other clinical indicators (Hazard ratio 10.85, 95% confidence interval 3.24–36.37, P < 0.0001, Table 4). In addition, significantly more N1 tumours had lost ARF expression compared with N0 tumours (81% [31/38] of N1 tumours *versus* 33.3% [3/9] of N0 tumours, Fisher's exact test P = 0.008).

ARF expression and gene methylation status in NE, BE and AC cell lines

We used carcinoma cell lines and immortalized cell lines of BE origin (Gohtert, Gihtert, Chtert), as well as an immortalized NE cell line (HET1A), to further investigate mechanisms leading to reduced ARF expression in BE and AC. Non-quantitative RT-PCR analyses (Fig. 2A, ARF) revealed loss of ARF expression in 3/6 carcinoma cell lines (SEG1, TE7, OC1), and retention of ARF expression in 3/3 BE cell lines, and in the NE cell line (HET1A). All GAPDH (glyceraldehyde phosphate dehydrogenase) controls were positive. Loss of ARF expression in SEG1, OC1 and TE7 did not occur by homozygous gene deletion, as PCR analysis of genomic DNA showed that ARF exon 1β and exon 2 sequences were present (Fig. 2A, exon 1ß, exon 2).

To determine how CpG island methylation of the ARF gene correlates with silencing of ARF in AC and BE, we carried out a methylation-specific PCR analysis (MSP) on bisulphite-treated genomic DNA derived from these cell lines (the amplified region, which falls within the 5′-UTR (untranslated region) and exon 1ß, is indicated by arrows in Fig. 2C). We found that normal oesophageal epithelial cells (HET1A) displayed only the unmethylated band, while all of the BE and carcinoma cell lines displayed both methylated and unmethylated bands (Fig. 2A, M, U). We have also observed lack of methylation of ARF in an additional cell line, BJ-1, derived from immortalized normal fibroblasts (not shown), adding additional support to the likelihood that methylation of this region in cultured

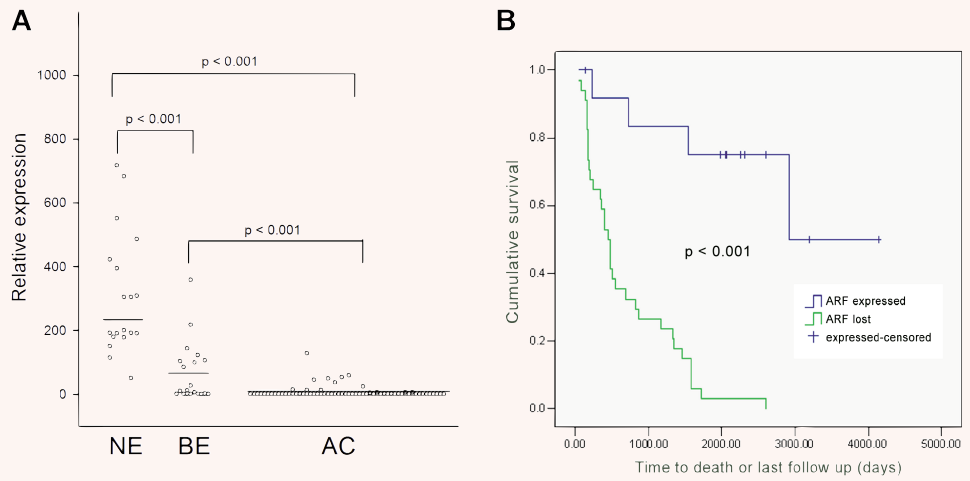

Fig. 1 Relative ARF expression in NE, BE and AC tissue specimens and correlation with patient survival. (**A**) Quantitative RT-PCR analysis of tissue specimens from normal oesophageal epithelium (NE, $n = 20$), Barrett's oesophagus (BE, $n = 20$) and oesophageal adenocarcinoma (AC, $n = 76$) using primers specific for ARF exon 1ß. ARF expression (average of triplicates) relative to glyceraldehyde phosphate dehydrogenase (GAPDH) is shown. Median values for each dataset are indicated by horizontal lines. The significance of the differences between datasets was evaluated by a Kruskal-Wallis rank sum test and P values are indicated above each pair of sets. (**B**) Kaplan–Meier survival curves of adenocarcinoma patients whose tumour either expressed ARF ($n = 13$) or lacked expression of ARF ($n = 34$). The difference between the curves was highly significant ($\chi^2 = 21.69$, d.f. = 1, $P < 0.001$, based on a Log-Rank Mantel-Cox test).

BE and carcinoma cell lines correlates with the disease process. Furthermore, a well-characterized colorectal carcinoma cell line, SW48 with methylated ARF [22–24] and no ARF expression [25], displayed only the M band (not shown), indicating that the presence of the M and U bands is not a universal feature of all cell lines. There are, nevertheless, several other published examples of monoallelic gene methylation. In particular, monoallelic methylation of the APC gene occurs in gastric mucosa associated with neoplastic lesions [26], and monoallelic methylation of the p16INK4a promoter in HCT116 colon cancer cells has been reported [27].

We ruled out cellular heterogeneity as a source of the methylated and unmethylated bands by showing that single cell-derived clones of the TE7 cell line (ARF—) were identical to the parental TE7 cell line with respect to ARF expression (Fig. 2B, ARF), and the presence of both methylated and unmethylated ARF bands following MSP analysis (Fig. 2B, M, U). A similar subcloning analysis (not shown) carried out on 5 subclones of the OC3 (ARF+) and OC1 (ARF—) cell lines confirmed that their respective subclones also resembled the parental line from which they were derived. The pattern of methylation observed in the parental lines therefore appears unlikely to represent a heterogeneous methylation pattern of ARF alleles within a mixed population of cells.

Bisulphite treatment converts unmethylated but not methylated cytosine to uracil and therefore generates a different sequence on methylated and unmethylated DNA. To rule out heterogeneity of CpG methylation across the ARF sequence as a source of the M and U bands, we carried out a direct sequence analysis of the MSP products (M and U bands) from bisulphite-treated genomic DNA of each of the nine cell lines shown in Figure 2A, using the same methylation-specific primers as were used in Figure 2A. The results, shown schematically in Figure 2C, show that the M band corresponds to a sequence methylated at more than 90% of the available CpG sites, whereas the U band corresponds to a completely unmethylated sequence.

A quantitative MSP analysis of bisulphite-treated genomic DNA using the MSP primers from Figure 2A, demonstrated that the two gene states are present in roughly equal amounts in all nine cell lines, consistent with a diploid gene dosage for ARF in these cell lines (Fig. 2D). To further confirm the presence of both methylated and unmethylated alleles of ARF in these cells, we carried out bisulphite sequencing of a 270 base pair region from minus 67 to plus 203 (relative to start of translation) of genomic DNA from OC3 cells using universal primers chosen so as to be complementary to 5′ and 3′ flanking regions without CpG sites. These primers were therefore insensitive to the methylation state of the amplified region and simultaneously amplified both methylated and unmethylated sequences with equal efficiency in one reaction. Figure 2D (right-hand panel) shows the results for a portion of the amplified region from +56 to +97, which includes 4 CpG sites and 6 isolated Cs. Bisulphite treatment converted all 6 isolated Cs to U (T), indicating a high efficiency of conversion. In contrast, for each C present in a

Table 3 Correlation of ARF expression and survival in AC patients ($n = 47$)

Differentiation	Sex	Age	T stage*	N stage*	DPR*	DPD*	Dead or alive at last follow-up	ΔCT*	Relative ARF expression*
Moderate	M	80	2	0	NR	4137	Alive	4.09	58.72
Poorly	M	74	2	1	NR	3188	Alive	4.76	36.91
Moderate	M	48	2	1	2918	2918	Dead	5.4	23.68
Moderate	M	44	3	1	2371	2602	Dead		N
Moderate	M	64	3	1	NR	2597	Alive	8.69	2.42
Moderate	M	56	1	0	NR	2313	Alive	4.36	48.70
Well	M	63	1	0	NR	2249	Alive	7.33	6.22
Well	M	78	1	0	NR	2060	Alive	6.15	14.08
Poorly	F	63	3	1	NR	2045	Alive	7.81	4.46
Moderate	M	66	2	1	NR	1984	Alive	8.57	2.63
Well	M	66	2	1	1576	1723	Dead		N
Well	M	70	2	1	1339	1583	Dead		N
Poorly	M	71	3	1	1550	1575	Dead		N
Poorly	M	76	3	1	1550	1575	Dead		N
Moderate	F	65	2	0	289	1533	Dead	8.82	2.21
Moderate	M	68	3	1	1450	1450	Dead		N
Moderate	F	51	3	0	1219	1339	Dead		N
Moderate	M	74	3	1	815	1327	Dead		N
Poorly	M	69	3	1	555	1172	Dead		N
Moderate	M	75	3	1	845	859	Dead		N
Poorly	F	73	3	1	566	816	Dead		N
Moderate	M	69	2	0	721	721	Dead	9.27	1.62
Poorly	M	56	2	1	524	687	Dead		N
Moderate	F	69	2	0	489	545	Dead		N
Poorly	M	74	2	1	449	510	Dead		N
Well	M	68	3	1	428	480	Dead		N
Poorly	M	51	3	1	357	477	Dead		N
Poorly	M	69	3	1	370	473	Dead		N
Poorly	M	47	3	1	277	446	Dead		N
Moderate	M	66	2	1	298	397	Dead		N
Poorly	M	NA	3	1	264	389	Dead		N
Poorly	M	53	3	1	317	347	Dead		N

Table 3 Continued

Differentiation	Sex	Age	T stage*	N stage*	DPR*	DPD*	Dead or alive at last follow-up	ΔCT*	Relative ARF expression*
Moderate	F	50	3	1	314	343	Dead		N
Poorly	F	74	3	1	153	238	Dead		N
Poorly	M	76	3	1	94	227	Dead	6.22	13.42
Well	M	48	3	1	118	207	Dead		N
Poorly	M	72	3	1	192	192	Dead		N
Moderate	M	46	3	1	129	176	Dead		N
Poorly	M	54	3	1	93	174	Dead		N
Poorly	F	69	2	1	101	169	Dead		N
Poorly	M	82	3	1	103	166	Dead		N
Poorly	M	50	3	1	118	166	Dead		N
Poorly	M	67	3	1	149	164	Dead		N
Moderate	M	89	2	1	92	132	Alive	9.77	1.15
Well	M	NA	1	0	129	129	Dead		N
Moderate	M	80	3	1	0	77	Dead		N
Poorly	M	50	2	1	41	41	Dead		N

*T stage = tumour stage; N stage = nodal status; DPR = days prior to relapse; NR = no relapse; DPD = days prior to death or last known alive; Relative ARF expression = $1000/2^{\Delta CT}$; $\Delta CT = CT_{ARF} - CT_{GAPDH}$; ($CT_{GAPDH}$ varied by <10% amongst samples); N = not measurable.

methylatable CpG sequence, bisulphite treatment gave rise to both a C and a U (T), as would be expected if only one of the two alleles were protected by methylation. Similar results were observed for the remainder of the sequence, and for Gihtert and SEG1 (not shown). Taken together, the results of the cell cloning analysis (Fig. 2B), the direct sequence analysis of MSP products (Fig. 2C), and the gene dosage analysis and bisulphite sequence analysis of genomic DNA (Fig. 2D), are highly suggestive of a stable pattern of CpG methylation of a single ARF allele in individual cells of BE or carcinoma origin.

Activation of ARF expression by 5-aza-2′-deoxycytidine

To demonstrate a functional role for the observed CpG methylation of ARF, we carried out an experiment with the DNA demethylating agent, 5-aza-2′-deoxycytidine (5-aza-CdR), followed by RT-PCR in the 3 BE cell lines and the 6 carcinoma cell lines (Fig. 3A). Treatment of cell lines with 1μM 5-aza-CdR for 24 hrs, followed by culturing for an additional 48 hrs, resulted in activation of ARF expression in the 3 carcinoma cell lines that had lacked ARF expression (SEG1, TE7, OC1, compare Figure 3A (ARF) and Figure 3A (ARF+aza)). GAPDH expression served as a control (Fig. 3A [GAPDH+aza]). This treatment also resulted in undetectable levels of CpG methylation of ARF in all 9 BE and carcinoma cell lines (Fig. 3A, M, U), evaluated by MSP. Furthermore, when Q-PCR was used to quantitate 5-aza-CdR-induced changes in ARF expression (relative to the GAPDH internal control) in the 3 BE cell lines (Go, Gi, Ch) and the 3 carcinoma cell lines that originally expressed ARF (OC3, FLO-1, OC33), we observed an approximate doubling of ARF expression levels (Fig. 3B), as expected if CpG methylation were to silence only one of the ARF alleles. Taken together, these results suggest that methylation silences the ARF allele on which it occurs, but do not explain how the unmethylated alleles are silenced in SEG1, TE7 and OC1 cells.

Correlation of histone H3 methylation with complete silencing of ARF

Histone H3 di and trimethylation on lysine 9 (K9), and di and trimethylation on lysine 27 (K27) have been implicated as important epigenetic mechanisms of gene silencing in cancer [28, 29].

Table 4 Variables in the Equation

		P value	Hazard ratio (95% confidence interval)
Step 1	Well differentiated	0.236	
	Moderately differentiated	0.671	1.33 (0.36–4.97)
	Poorly differentiated	0.178	2.32 (0.68–7.93)
	T1	0.969	
	T2	0.823	1.382 (0.08–23.40)
	T3	0.841	1.10 (0.44–2.72)
	N stage	0.548	1.47 (0.42–5.10)
	ARF expression lost	0.001	13.54 (2.93–62.43)
Step 2	Well differentiated	0.228	
	Moderately differentiated	0.731	1.21 (0.41–3.61)
	Poorly differentiated	0.149	2.15 (0.76–6.05)
	N stage	0.449	1.55 (0.50–4.86)
	ARF expression lost	<0.001	12.31 (3.33–45.49)
Step 3	Well differentiated	0.283	
	Moderately differentiated	0.625	1.30 (0.450–3.79)
	Poorly differentiated	0.174	2.03 (0.73–5.65)
	ARF expression lost	<0.001	10.53 (3.08–35.99)
Step 4	ARF expression lost	<0.001	10.85 (3.24–36.37)

Multivariate Cox regression model using a backwards stepwise method. Differentiation, T-stage, N-Stage and ARF expression were entered into the model with only ARF expression remaining (Hazard ratio 10.85, 95% confidence interval 3.24–36.37, $P < 0.0001$).

We therefore carried out a Chromatin Immunoprecipitation (ChIP) analysis using an antibody specific for histone H3 trimethylated lysine 9 (H3-K9-Me3), or using an antibody with dual specificity for the dimethylated form of histone H3 lysine K9 (H3-K9-Me2) and the di and trimethylated forms of lysine 27 (H3-K27-Me), followed by PCR analysis of the associated ARF sequences, to investigate the presence of this modification on ARF alleles in the series of cell lines examined above. As shown in Figure 3C, the ARF gene was found to be associated with chromatin containing histone H3-K9-Me3, H3-K9-Me2 and H3-K27Me only in the three carcinoma cell lines, SEG1, TE7 and OC1 (Fig. 3C), in which complete ARF gene silencing occurred. In all other cell lines, namely the three BE cell lines (Go, Gi, Ch), and three of the carcinoma cell lines (OC3, FLO-1, OC33) where partial silencing of ARF through CpG methylation was observed, there was no evidence for histone methylation (Fig. 3C). Input ARF levels were the same in all cases (Fig. 3C, ARF input). Controls (no antibody) were negative in all cases (not shown). The results suggest that histone methylation-induced silencing of ARF could also predispose to malignant transformation and to disease progression in AC.

Association of methylated histone H3 with unmethylated ARF DNA

To determine whether histone methylation occurs on both DNA methylated and DNA unmethylated alleles of ARF, we carried out a further MSP analysis of the DNA isolated from the histone-antibody immunoprecipitated material and treated with bisulphite. We found that the ARF allele associated with histone H3-K9-Me3, histone H3-K9-Me2 or with histone H3-K27-Me in SEG1, TE7, and OC1 cells is unmethylated at CpG sites (Fig. 3C, M, U). Nevertheless, treatment of SEG1, TE7, and OC1 cells with the DNA demethylating agent, 5-aza-CdR, resulted in a complete reversal of these methylated histone modifications, as revealed by ChIP analysis, even though that allele lacked CpG island methylation (Fig. 3D), consistent with a previous report [29, 30]. Input ARF levels were the same in all cases (Fig. 3D, ARF input+aza), and controls (no-antibody) were negative (not shown). The results indicate that CpG methylation and histone H3 methylation occur in a mutually exclusive manner on the ARF gene in adenocarcinoma cell lines, and that each can be independently reversed by 5-aza-CdR.

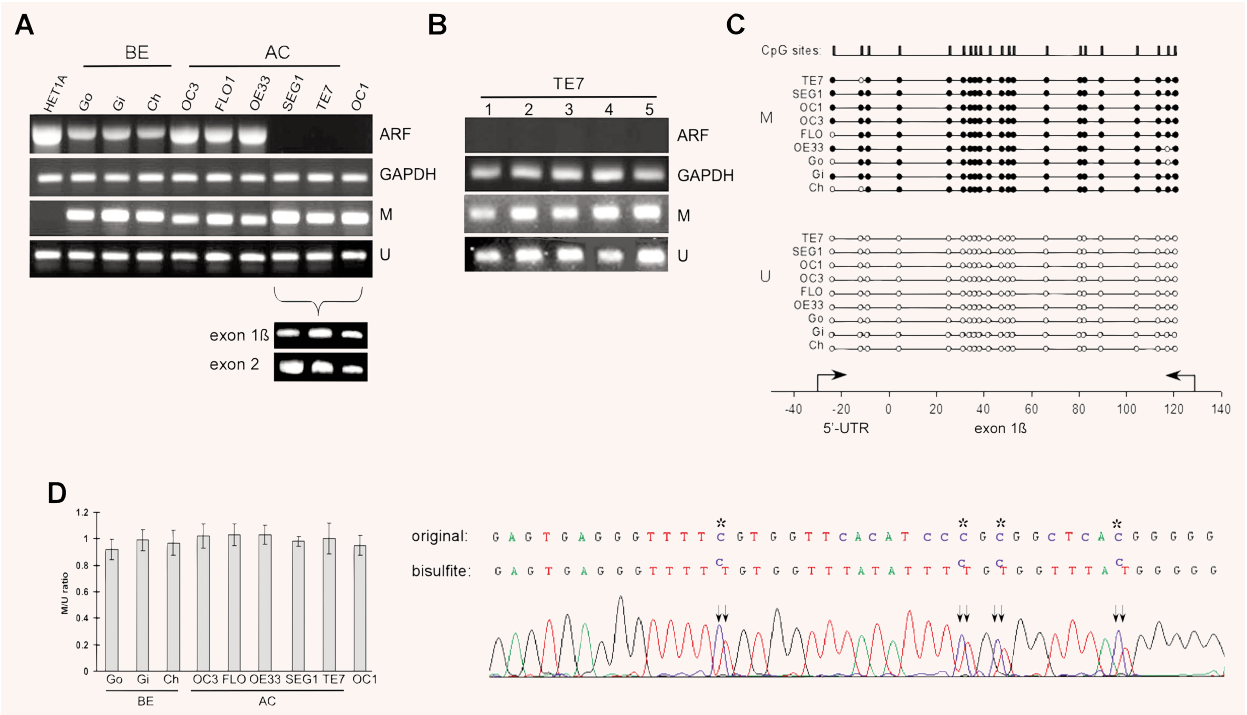

Fig. 2 ARF expression and gene methylation status in NE, BE and carcinoma cell lines. (**A**) RT-PCR analysis of ARF expression (ARF) and GAPDH expression (GAPDH) in the normal oesophageal epithelial cell line, HET1A, in the BE cell lines Gohtert (Go), Gihtert (Gi) and Chtert (Ch), in the AC cell lines OC3, FLO-1, OE33, SEG1, TE7 and in the oesophageal squamous cell carcinoma cell line, OC1. MSP analysis using methylated-specific (M) and unmethylated-specific (U) primers for the 5′-UTR/exon 1β region of the ARF gene in the same series of cell lines. Triplicate repeats produced similar results. (Lower panel) PCR analysis of genomic DNA from SEG1, TE7 and OC1 using primers for ARF exon 1ß (top row), and ARF exon 2 (lower row). (**B**) RT-PCR analysis of ARF expression (ARF) and GAPDH expression (GAPDH) of 5 subclones of the TE7 cell line. Triplicate repeats produced similar results. (**C**) (Top) Schematic representation of CpG sites along the 5′-UTR and exon 1ß region of the ARF gene. (Middle) Schematic representation of locations of methylated CpG sites (●) and unmethylated CpG sites (●) obtained by direct sequencing of the MSP products (M and U bands) from the indicated BE and carcinoma cells lines, amplified with methylated-specific primers (M) or unmethylated-specific primers (U). (Bottom) Positions along the ARF sequence of forward (↦) and reverse (↤) primers used for MSP analysis. '0' represents the start of translation. (**D**) Quantitative MSP analysis of ARF in genomic DNA from BE and carcinoma cell lines. Bars represent the average M/U ratios of triplicate assays, with standard deviations shown. (Right panel) Bisulphite-generated sequence profile of a representative region of the ARF gene from OC3 cells. Original and bisulphite-generated sequences are shown above the sequence profile. Asterisks indicate CpG sites. Doublet arrows indicate locations where both C and T appear in the bisulphite-generated sequence.

Discussion

This study demonstrates that the transition from normal oesophageal epithelium to BE to AC correlates with a progressive decrease in ARF expression. Complete silencing of ARF was found in 75% in the AC specimens, and correlated with poor prognosis. In our dataset, univariate analysis revealed that ARF expression was prognostically significant and in fact outperformed all other clinical variables in a multivariate analysis. The results support an important role for ARF in suppressing oesophageal cancer, and suggest that loss of ARF expression could provide a useful prognostic indicator.

Loss of p16INK4a expression (deletion, silencing, mutation) has been found in over 70% of BE patients [31], and because it shares its exon 2 region with ARF (reviewed in [32]), deletions or mutations in this region could, in principle, affect both genes, and obscure the respective roles of each gene in cancer. However, there are several reasons why abnormalities in the two genes may not correlate. First, the exon 2 region is read in an alternate reading frame for p16INK4a and ARF, so mutations in this region do not necessarily affect both proteins. Second, the first exon of ARF, which retains tumour suppressor activity [33], is expressed from a unique promoter, and it located some 20 kilobases upstream of the first exon of the p16INK4A gene, so deletion or methylation of one of the genes can occur without affecting the other, and this has been documented [34–36]. Our preliminary studies on a small sample set of BE specimens suggests that ARF and p16INK4a abnormalities arise independently of each other in pre-malignant lesions, but a further full scale study is needed to confirm this.

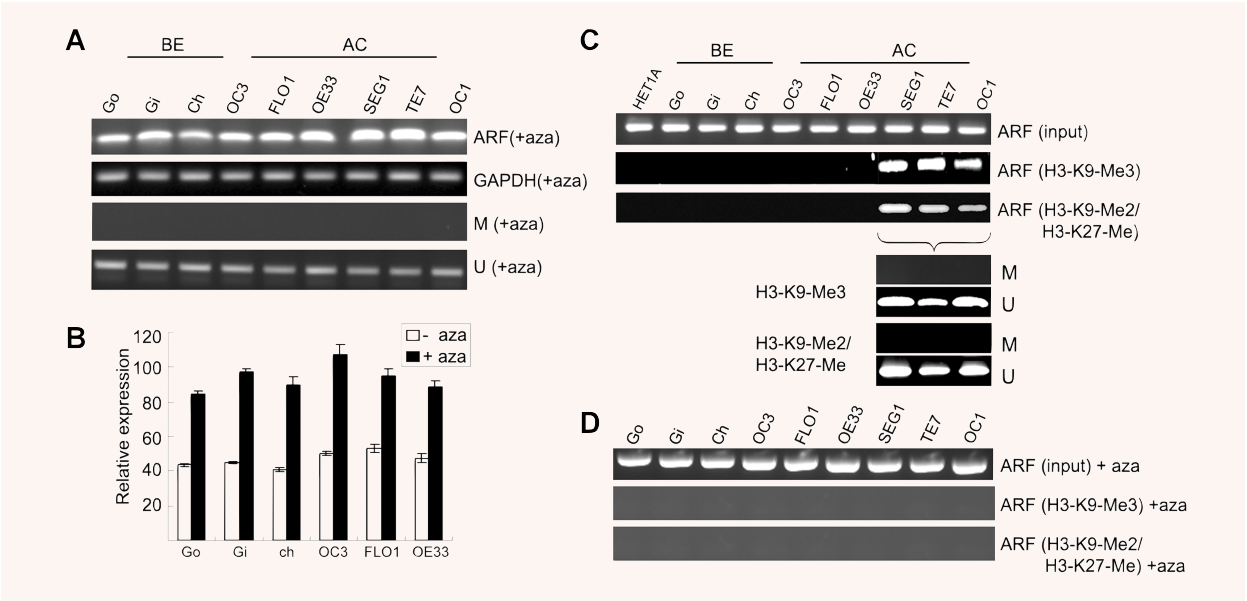

Fig. 3 Epigenetic changes affecting the ARF gene and associated histones in BE and carcinoma cell lines, and responses to 5-aza-CdR treatment. (**A**) RT-PCR analysis of ARF expression (ARF+aza) and GAPDH expression (GAPDH+aza) in the indicated BE and carcinoma cell lines after treatment with 5-aza-CdR. MSP analysis using methylated-specific (M+aza) and unmethylated-specific (U+aza) primers for the 5′-UTR/exon 1β region of the ARF gene in the same series of cell lines after treatment with 5-aza-CdR. (**B**) Quantitation by Q-PCR of 5-aza-CdR-induced changes in ARF expression (relative to GAPDH internal control) in the 3 BE cell lines and the 3 carcinoma cell lines that originally expressed ARF (bars represent averages of triplicate assays, with standard deviations shown). (**C**) ChIP analysis of ARF 5′-UTR/exon 1ß DNA sequences associated with histone H3 lysine 9 trimethylation (ARF H3-K9-Me3) and histone H3 lysine 9 dimethylation + lysine 27 methylation (ARF H3-K9-Me2/H3-K9-27-Me) in BE and carcinoma cell lines prior to treatment with 5-aza-CdR. Input DNA (ARF input) serves as a control. Lower panels show MSP analysis of ARF DNA sequences associated with histone H3 lysine 9 trimethylation (M,U) and histone H3 lysine 9 dimethylation + lysine 27 methylation (M,U) in SEG1, TE7, and OC1 cells. (**D**) ChIP analysis carried out on BE and carcinoma cell lines as in panel C, after treatment with 5-aza-CdR. Analyses were repeated 2–3 times with independent preparations to confirm reproducibility.

Loss of wild-type p53 expression occurs in some 50–70% patients with BE and AC, and correlates with increased aneuploidy [37], increased risk of progression [37], and with poor prognosis [38]. In our analysis of BE specimens, complete loss of ARF expression occurred in some 20% of BE specimens and 75% of AC specimens, indicating that its occurrence was frequent and likely to occur in many specimens simultaneously with mutation or deletion of p53. ARF plays a well-described role in the p53 pathway and in certain cancers [39, 40], a reciprocal pattern of abnormalities has been observed for p53 and ARF, consistent with their action in a common pathway. However, the high frequency of both abnormalities in oesophageal cancer suggests that the two abnormalities contribute independently to disease progression in this disease, and is consistent with published evidence of a p53-independent activity for ARF in mammalian cells [41, 42].

CpG methylation is a common mechanism of tumour suppressor gene silencing in cancer [15], and CpG methylation of the first exon and proximal promoter of ARF is well documented in other cancers and cancer-derived cell lines [43, 44]. Methylation of lysines 9 and 27 of the N-terminal domain of histone H3, is also a mark of silenced genes and aberrant methylation of these residues has been implicated in gene silencing in cancer [28, 29]. CpG methylation can be associated with histone H3 methylation of K9 and K27, and epigenetic changes at the level of DNA and histone can cooperate in gene silencing [45]. However, long-range epigenetic silencing of gene expression due solely to histone methylation without DNA methylation has also been described [46]. Our results suggest that either DNA or histone H3 methylation can provide the primary mechanism of ARF gene silencing in oesophageal cancer, and that each appears to be sufficient to maintain stable silencing. The TE7 cell line we have used has recently been reported to be of squamous cell carcinoma origin [47], but was still considered to be a useful addition to our panel of lines to determine the mechanism of silencing, however.

Consistent with an earlier study [29], we find that both DNA and histone methylations are reversible with 5-aza-CdR, and that this treatment reactivates ARF expression. These results provide additional rationale for the clinical application of demethylating agents such as 5-aza-cytidine or 5-aza-2′-deoxycytidine [48], or for specific histone demethylating approaches [28] to prevent tumourigenic transformation of pre-malignant lesions and possibly to reverse oesophageal malignancy.

Acknowledgements

The clinical part of this work would not have been possible without the help of endoscopy staff and patients. The authors would especially like to thank the clinicians who collected specimens for this study: Professor Derek Alderson, Professor Hugh Barr, Dr. Laurence Lovat and the histopathologists who verified the diagnoses: Dr. Vicki Save, Professor Marco Novelli, Professor Neil Shepherd and Professor Bryan Warren. This work was supported by grants (to RAG) from the NIH/NCI (CA 111868) and the California Tobacco-Related Disease Research Program (11RT-0074), and (to RCF) from the Medical Research Council of the United Kingdom. The authors declare that no conflicts of interest exist.

References

1. **Polednak AP.** Trends in survival for both histologic types of esophageal cancer in US surveillance, epidemiology and end results areas. *Int J Cancer*. 2003; 105: 98–100.
2. **Shaheen N, Ransohoff DF.** Gastroesophageal reflux, barrett esophagus, and esophageal cancer: scientific review. *JAMA*. 2002; 287: 1972–81.
3. **Brabender J, Marjoram P, Salonga D, Metzger R, Schneider PM, Park JM, Schneider S, Holscher AH, Yin J, Meltzer SJ, Danenberg KD, Danenberg PV, Lord RV.** A multigene expression panel for the molecular diagnosis of Barrett's esophagus and Barrett's adenocarcinoma of the esophagus. *Oncogene*. 2004; 23: 4780–8.
4. **Lao-Sirieix P, Lovat L, Fitzgerald RC.** Cyclin A immunocytology as a risk stratification tool for Barrett's esophagus surveillance. *Clin Cancer Res*. 2007; 13: 659–65.
5. **Maley CC, Galipeau PC, Finley JC, Wongsurawat VJ, Li X, Sanchez CA, Paulson TG, Blount PL, Risques RA, Rabinovitch PS, Reid BJ.** Genetic clonal diversity predicts progression to esophageal adenocarcinoma. *Nat Genet*. 2006; 38: 468–73.
6. **Dolan K, Morris AI, Gosney JR, Field JK, Sutton R.** Loss of heterozygosity on chromosome 17p predicts neoplastic progression in Barrett's esophagus. *J Gastroenterol Hepatol*. 2003; 18: 683–9.
7. **Galipeau PC, Li X, Blount PL, Maley CC, Sanchez CA, Odze RD, Ayub K, Rabinovitch PS, Vaughan TL, Reid BJ.** NSAIDs modulate CDKN2A, TP53, and DNA content risk for progression to esophageal adenocarcinoma. *PLoS Med*. 2007; 4: e67.
8. **Rabinovitch PS, Longton G, Blount PL, Levine DS, Reid BJ.** Predictors of progression in Barrett's esophagus III: baseline flow cytometric variables. *Am J Gastroenterol*. 2001; 96: 3071–83.
9. **Kamb A, Gruis NA, Weaver-Feldhaus J, Liu Q, Harshman K, Tavtigian SV, Stockert E, Day RS 3rd, Johnson BE, Skolnick MH.** A cell cycle regulator potentially involved in genesis of many tumor types. *Science*. 1994; 264: 436–40.
10. **Sherr CJ.** Tumor surveillance *via* the ARF-p53 pathway. *Genes Dev*. 1998; 12: 2984–91.
11. **Gazzeri S, Della Valle V, Chaussade L, Brambilla C, Larsen CJ, Brambilla E.** The human p19ARF protein encoded by the beta transcript of the p16INK4a gene is frequently lost in small cell lung cancer. *Cancer Res*. 1998; 58: 3926–31.
12. **Saadatmandi N, Tyler T, Huang Y, Haghighi A, Frost G, Borgstrom P, Gjerset RA.** Growth suppression by a p14(ARF) exon 1beta adenovirus in human tumor cell lines of varying p53 and Rb status. *Cancer Gene Ther*. 2002; 9: 830–9.
13. **Sanchez-Cespedes M, Reed AL, Buta M, Wu L, Westra WH, Herman JG, Yang SC, Jen J, Sidransky D.** Inactivation of the INK4A/ARF locus frequently coexists with TP53 mutations in non-small cell lung cancer. *Oncogene*. 1999; 18: 5843–9.
14. **Weber JD, Jeffers JR, Rehg JE, Randle DH, Lozano G, Roussel MF, Sherr CJ, Zambetti GP.** p53-independent functions of the p19(ARF) tumor suppressor. *Genes Dev*. 2000; 14: 2358–65.
15. **Jones PA, Baylin SB.** The fundamental role of epigenetic events in cancer. *Nat Rev Genet*. 2002; 3: 415–28.
16. **Esteller M, Cordon-Cardo C, Corn PG, Meltzer SJ, Pohar KS, Watkins DN, Capella G, Peinado MA, Matias-Guiu X, Prat J, Baylin SB, Herman JG.** p14ARF silencing by promoter hypermethylation mediates abnormal intracellular localization of MDM2. *Cancer Res*. 2001; 61: 2816–21.
17. **Vieth M, Schneider-Stock R, Rohrich K, May A, Ell C, Markwarth A, Roessner A, Stolte M, Tannapfel A.** INK4a-ARF alterations in Barrett's epithelium, intraepithelial neoplasia and Barrett's adenocarcinoma. *Virchows Arch*. 2004; 445: 135–41.
18. **Wong DJ, Paulson TG, Prevo LJ, Galipeau PC, Longton G, Blount PL, Reid BJ.** p16(INK4a) lesions are common, early abnormalities that undergo clonal expansion in Barrett's metaplastic epithelium. *Cancer Res*. 2001; 61: 8284–9.
19. **Barrett MT, Pritchard D, Palanca-Wessels C, Anderson J, Reid BJ, Rabinovitch PS.** Molecular phenotype of spontaneously arising 4N (G2-tetraploid) intermediates of neoplastic progression in Barrett's esophagus. *Cancer Res*. 2003; 63: 4211–7.
20. **Rockett JC, Larkin K, Darnton SJ, Morris AG, Matthews HR.** Five newly established oesophageal carcinoma cell lines: phenotypic and immunological characterization. *Br J Cancer*. 1997; 75: 258–63.
21. **Su M, Chin SF, Li XY, Edwards P, Caldas C, Fitzgerald RC.** Comparative genomic hybridization of esophageal adenocarcinoma and squamous cell carcinoma cell lines. *Dis Esophagus*. 2006; 19: 10–4.
22. **Gayet J, Zhou XP, Duval A, Rolland S, Hoang JM, Cottu P, Hamelin R.** Extensive characterization of genetic alterations in a series of human colorectal cancer cell lines. *Oncogene*. 2001; 20: 5025–32.
23. **Toyota M, Ahuja N, Ohe-Toyota M, Herman JG, Baylin SB, Issa JP.** CpG island methylator phenotype in colorectal cancer. *Proc Natl Acad Sci USA*. 1999; 96: 8681–6.
24. **Zheng S, Chen P, McMillan A, Lafuente A, Lafuente MJ, Ballesta A, Trias M, Wiencke JK.** Correlations of partial and extensive methylation at the p14(ARF) locus with reduced mRNA expression in colorectal cancer cell lines and clinicopathological features in primary tumors. *Carcinogenesis*. 2000; 21: 2057–64.
25. **Fini L, Selgrad M, Fogliano V, Graziani G, Romano M, Hotchkiss E, Daoud YA, De Vol EB, Boland CR, Ricciardiello L.** Annurca apple polyphenols have potent demethylating activity and can reactivate silenced tumor suppressor genes in colorectal cancer cells. *J Nutr*. 2007; 137: 2622–8.
26. **Clement G, Bosman FT, Fontolliet C, Benhattar J.** Monoallelic methylation of

the APC promoter is altered in normal gastric mucosa associated with neoplastic lesions. *Cancer Res*. 2004; 64: 6867–73.

27. **Myohanen SK, Baylin SB, Herman JG.** Hypermethylation can selectively silence individual p16ink4A alleles in neoplasia. *Cancer Res*. 1998; 58: 591–3.
28. **Abbosh PH, Montgomery JS, Starkey JA, Novotny M, Zuhowski EG, Egorin MJ, Moseman AP, Golas A, Brannon KM, Balch C, Huang TH, Nephew KP.** Dominant-negative histone H3 lysine 27 mutant derepresses silenced tumor suppressor genes and reverses the drug-resistant phenotype in cancer cells. *Cancer Res*. 2006; 66: 5582–91.
29. **Nguyen CT, Weisenberger DJ, Velicescu M, Gonzales FA, Lin JC, Liang G, Jones PA.** Histone H3-lysine 9 methylation is associated with aberrant gene silencing in cancer cells and is rapidly reversed by 5-aza-2′-deoxycytidine. *Cancer Res*. 2002; 62: 6456–61.
30. **Takebayashi S, Nakao M, Fujita N, Sado T, Tanaka M, Taguchi H, Okumura K.** 5-Aza-2′-deoxycytidine induces histone hyperacetylation of mouse centromeric heterochromatin by a mechanism independent of DNA demethylation. *Biochem Biophys Res Commun*. 2001; 288: 921–6.
31. **Maley CC, Galipeau PC, Li X, Sanchez CA, Paulson TG, Blount PL, Reid BJ.** The combination of genetic instability and clonal expansion predicts progression to esophageal adenocarcinoma. *Cancer Res*. 2004; 64: 7629–33.
32. **Gallagher SJ, Kefford RF, Rizos H.** The ARF tumour suppressor. *Int J Biochem Cell Biol*. 2006; 38: 1637–41.
33. **Kamijo T, Weber JD, Zambetti G, Zindy F, Roussel MF, Sherr CJ.** Functional and physical interactions of the ARF tumor suppressor with p53 and Mdm2. *Proc Natl Acad Sci USA*. 1998; 95: 8292–7.
34. **Tsujimoto H, Hagiwara A, Sugihara H, Hattori T, Yamagishi H.** Promoter methylations of p16INK4a and p14ARF genes in early and advanced gastric cancer. Correlations of the modes of their occurrence with histologic type. *Pathol Res Pract*. 2002; 198: 785–94.
35. **Viswanathan M, Tsuchida N, Shanmugam G.** Selective deletion of p14(ARF) exon 1beta of the INK4a locus in oral squamous cell carcinomas of Indians. *Oral Oncol*. 2001; 37: 341–4.
36. **Weber A, Bellmann U, Bootz F, Wittekind C, Tannapfel A.** INK4a-ARF alterations and p53 mutations in primary and consecutive squamous cell carcinoma of the head and neck. *Virchows Arch*. 2002; 441: 133–42.
37. **Galipeau PC, Cowan DS, Sanchez CA, Barrett MT, Emond MJ, Levine DS, Rabinovitch PS, Reid BJ.** 17p (p53) allelic losses, 4N (G2/tetraploid) populations, and progression to aneuploidy in Barrett's esophagus. *Proc Natl Acad Sci USA*. 1996; 93: 7081–4.
38. **Schneider PM, Stoeltzing O, Roth JA, Hoelscher AH, Wegerer S, Mizumoto S, Becker K, Dittler HJ, Fink U, Siewert JR.** P53 mutational status improves estimation of prognosis in patients with curatively resected adenocarcinoma in Barrett's esophagus. *Clin Cancer Res*. 2000; 6: 3153–8.
39. **Pomerantz J, Schreiber-Agus N, Liegeois NJ, Silverman A, Alland L, Chin L, Potes J, Chen K, Orlow I, Lee HW, Cordon-Cardo C, DePinho RA.** The Ink4a tumor suppressor gene product, p19Arf, interacts with MDM2 and neutralizes MDM2's inhibition of p53. *Cell*. 1998; 92: 713–23.
40. **Zhang Y, Xiong Y, Yarbrough WG.** ARF promotes MDM2 degradation and stabilizes p53: ARF-INK4a locus deletion impairs both the Rb and p53 tumor suppression pathways. *Cell*. 1998; 92: 725–34.
41. **Ayrault O, Andrique L, Larsen CJ, Seite P.** The negative regulation of ribosome biogenesis: a new Arf-dependent pathway controlling cell proliferation? *Med Sci*. 2006; 22: 519–24.
42. **Sherr CJ, Bertwistle D, W DENB, Kuo ML, Sugimoto M, Tago K, Williams RT, Zindy F, Roussel MF.** p53-dependent and -independent functions of the Arf tumor suppressor. *Cold Spring Harb Symp Quant Biol*. 2005; 70: 129–37.
43. **Esteller M, Tortola S, Toyota M, Capella G, Peinado MA, Baylin SB, Herman JG.** Hypermethylation-associated inactivation of p14(ARF) is independent of p16(INK4a) methylation and p53 mutational status. *Cancer Res*. 2000; 60: 129–33.
44. **Robertson KD, Jones PA.** The human ARF cell cycle regulatory gene promoter is a CpG island which can be silenced by DNA methylation and down-regulated by wild-type p53. *Mol Cell Biol*. 1998; 18: 6457–73.
45. **Schlesinger Y, Straussman R, Keshet I, Farkash S, Hecht M, Zimmerman J, Eden E, Yakhini Z, Ben-Shushan E, Reubinoff BE, Bergman Y, Simon I, Cedar H.** Polycomb-mediated methylation on Lys27 of histone H3 pre-marks genes for *de novo* methylation in cancer. *Nat Genet*. 2007; 39: 232–6.
46. **Stransky N, Vallot C, Reyal F, Bernard-Pierrot I, de Medina SG, Segraves R, de Rycke Y, Elvin P, Cassidy A, Spraggon C, Graham A, Southgate J, Asselain B, Allory Y, Abbou CC, Albertson DG, Thiery JP, Chopin DK, Pinkel D, Radvanyi F.** Regional copy number-independent deregulation of transcription in cancer. *Nat Genet*. 2006; 38: 1386–96.
47. **Boonstra JJ, van der Velden AW, Beerens EC, van Marion R, Morita-Fujimura Y, Matsui Y, Nishihira T, Tselepis C, Hainaut P, Lowe AW, Beverloo BH, van Dekken H, Tilanus HW, Dinjens WN.** Mistaken identity of widely used esophageal adenocarcinoma cell line TE-7. *Cancer Res*. 2007; 67: 7996–8001.
48. **Wijermans PW, Krulder JW, Huijgens PC, Neve P.** Continuous infusion of low-dose 5-Aza-2′-deoxycytidine in elderly patients with high-risk myelodysplastic syndrome. *Leukemia*. 1997; 11: 1–5.